Simulation of Homogeneous Condensation of Ethanol in High Pressure Supersonic Nozzle Flows using BGK Condensation Model

Rakesh Kumar and D. A. Levin

Pennsylvania State University, University Park, PA 16802

Abstract. In the present work, we have simulated the homogeneous condensation flow of ethanol using the Bhatnagar-Gross-Krook (BGK) based condensation model for the experimental conditions of Wegener *et al.* [1]. In an earlier work carried out by Gallagher-Rogers *et al.* [2], it was found not possible to simulate the experimental conditions using the direct simulation Monte-Carlo (DSMC) based condensation model. In this work we use a statistical-BGK approach to model condensation and compare our simulated predictions of the point of condensation onset and the distribution of mass fraction along the nozzle centerline with experiments. The experiments provide data for different cases corresponding to varying amounts of ethanol concentration, compared to air, for total mixture pressures which remains mostly constant for all cases. Our numerical results show good agreement with the experiments, thus validating our BGK based condensation model for high pressure flow applications.

Keywords: Homogeneous condensation of ethanol, Statistical BGK method
PACS: 05.20.Jj

INTRODUCTION

Homogeneous condensation occurs when a gas becomes supersaturated, leading to the formation of clusters in the flowfield as gas particles are consumed. It is interesting to understand the effects of condensation on the rarefied flow surrounding spacecraft and the plume radiation signature of supersonic expansions to vacuum. Rochelle *et al.* [3] studied the effects of cluster particles in the plume on its impingement on the International Space Station components and found that they caused abnormal heating, unbalanced surface pressure distributions, and moreover contamination. These phenomena can adversely affect the life span of important spacecraft components. Gimelshein *et al.* [4] found that the ultraviolet radiation intensity at 230 nm increases by a factor of 300 due to the presence of cluster particles in the plume of an aluminized solid propellant. In the present work, we are focusing on the homogeneous condensation of ethanol, since its physical properties are similar to those of hydrazine, a commonly used propellant for attitude control thrusters. Ethanol was used to model hydrazine in the experiments of Yarygin *et al.* [5], who used model thrusters in a vacuum chamber to test the effectiveness of screens in blocking contaminants from reaching the backflow area of the plume. Many other laboratory experiments have been carried out to determine the onset of condensation in ethanol in supersonic nozzles [1, 6, 7, 8].

In our previous work on ethanol condensation, Gallagher-Rogers *et al.* [2] modeled the homogeneous condensation of ethanol in a supersonic nozzle expansion using the classical nucleation theory (CNT) in the DSMC framework. The goal of that research[2] was to compare the condensation onset with the experimental data of Wegener *et al.* [1]. However, it was found that a pure DSMC approach could not model the experimental conditions of Ref. [1]. Instead, to make the calculations tractable, the experimental conditions that were simulated were modified. For example, the previous simulation of Case 1, given in Table 1, was performed assuming that the total mixture pressure was that of the pure ethanol pressure actually used in the experiments. The table shows that the maximum total pressure in the experiment was 83.46 kPa, which is simply too computationally challenging for a pure DSMC simulation. Thus the maximum pressure simulated in the work of Ref. [2] was only for a pressure of 1.87 kPa as compared with the actual experimental value of 83.46 kPa.

In our recent work, we developed a condensation model in the statistical BGK framework [9] that was found to be numerically more efficient, but as accurate as the DSMC method. This work enabled us to extend our condensation research to higher density, non-equilibrium expanding flows. The condensation model takes into account the processes of nucleation, cluster-monomer sticking and non-sticking collisions, cluster-cluster coalescence, and evaporation. We obtained good agreement with experiments [10] in terms of cluster number density and size as well as gas rotational temperature variation along the freely expanding plume centerline [9]. More recently, we implemented a new weighting scheme in our BGK based condensation model [11]. It was found that the use of the new weighting scheme made the method numerically more efficient and in turn allowed simulations of higher pressure condensation flows or those flows where the condensible gas and/or condensate is a trace species. In the present work, we continue our

studies by simulating condensation flows of ethanol for the experimental conditions of Wegener *et al.* [1]. We apply the statistical BGK based condensation model to model the experimental data for homogeneous condensation of ethanol in a supersonic nozzle [1]. The experimental data that was obtained by Wegener *et al.* [1] consists of measurements of condensation onset and the mass fraction of condensed ethanol along the nozzle centerline for different supply mass fractions of ethanol in dry air, ω, as shown in Table 1. It was observed in the experiments that in all of the cases, almost all of the ethanol condensed inside the nozzle. We will compare our results with the experiments in terms of condensed ethanol mass fraction distribution and the location of condensation onset, which in this work is defined as the point at which the condensed mass fraction reaches 10^{-3}, as it was in Wegener *et al.* [1].

The outline of the remainder of the paper is as follows. The next section is devoted to a brief discussion about the numerical method used in the present work. Results of the current work are then compared with experiments and finally we present our conclusions.

COMPUTATIONAL METHOD

In the present work, we use a statistical BGK based condensation model to simulate expanding flow through a nozzle undergoing homogeneous condensation. The BGK method is a technique that approximates the solution of the Boltzmann equation, which is the most general equation of fluid flow.

$$\frac{\partial}{\partial t}(nf) + v \cdot \frac{\partial}{\partial \vec{r}}(nf) + \vec{F} \cdot \frac{\partial}{\partial \vec{v}}(nf) = \int_{-\infty}^{\infty} \int_{0}^{4\pi} n^2 \left(f^* f_1^* - f f_1\right) v_r \sigma d\Omega d\vec{v} \tag{1}$$

where f and f_1 are the pre-collision single particle velocity distribution functions of the two colliding particles and f^* and f_1^* are their post-collision velocity distribution functions; $\vec{F}$ is an external force per unit mass applied to the particles (assumed to be zero for the present study); σ is the differential cross-section of the binary collision and Ω is the solid angle; v_r is the relative velocity of the colliding particles, and n is the number density.

It can be seen that the collision term on the right hand side of the Boltzmann equation, Eq.(1), involves multiple integrations in its formulation, making it difficult to compute. Different simplified models have been proposed to model this complicated collision term with one such simplified model expressing the collision term in a relaxation form known as the Bhatnagar-Gross-Krook (BGK) model:

$$\left[\frac{\partial}{\partial t}(nf)\right]_{collision} = \nu n (f_e - f) \tag{2}$$

where n is the number density, ν is the characteristic relaxation frequency, and f_e is the Maxwellian distribution function.

With this approximation, the Bhatnagar-Gross-Krook (BGK) model simplifies the nonlinear collision term of the Boltzmann equation without modeling individual collisions. This simplification is reasonable for flows with large numbers of collisions since the details of the particle interactions are not significant in reproducing most of the experimentally measured macroscopic quantities such as temperature, pressure, or flow velocity, if the collision rate is sufficiently high[12]. Because the BGK equation reproduces correct moments and satisfies the H-theorem for entropy production, it is accepted as an accurate physical model of high density flows such as those under consideration in the present work. More details about the method can be found in Refs. [13, 14, 15].

In the previous work of the authors [14, 16, 15], the statistical BGK method was implemented in the SMILE[17] DSMC computational tool. A comparative study of the DSMC and statistical BGK method was carried out in Ref. [14] by simulating a supersonic expansion of argon to vacuum in a nozzle for different pressure cases and comparing with the DSMC solution as the benchmark. The statistical BGK method was found to be in good agreement with the benchmark DSMC method. It was also shown that the statistical method of solving the BGK equation was four times more numerically efficient than the deterministic finite volume BGK method and twice as efficient as the DSMC method. Another comparative study was carried out in Ref. [18] to estimate the accuracy of the statistical BGK method for a multiple species case. The study involved modeling of RCC crack growth using the kinetic BGK method for internal and external flows. The method was found to be in good agreement with the DSMC method for the external flows. For modeling the local high pressure flows within the vicinity of a crack, only the statistical BGK method was applied, because of its cost effectiveness over the DSMC method.

After the successful validation of statistical BGK method, a new condensation model was incorporated in the BGK framework. The model is based on classical nucleation theory (CNT) and involves the processes of nucleation, condensation, coalescence and evaporation. In this work, the model is modified so as to be used for ethanol. A new weighting scheme that was recently developed and validated [11] is used that makes the method more efficient and in turn allows the simulation of computationally more challenging flows such as that studied in this work. Detailed descriptions of the BGK based models for the aforesaid processes and the new weighting scheme can be found in Refs. [9, 11].

VALIDATION RESULTS FOR THE CONDENSATION MODEL IN THE STATISTICAL BGK FRAMEWORK

Now we present and discuss the results for the condensation flow of ethanol at a stagnation temperature and a pressure of 296 K and 83 kPa, respectively, with air as the carrier gas. The two cases considered here correspond to ethanol supply mass fractions of 0.008 and 0.005, as shown in Table 1. Table 2 shows the variation of ethanol properties, such as saturation pressure and surface tension, with temperature that were used in this work. Ethanol is assumed to have three rotational degrees of freedom and inactivated vibrational modes due to the operating temperatures ($\sim$240K) being very low compared to its characteristic vibrational temperature, 2533.5 K. To reduce the computational cost, a two dimensional axisymmetric scheme was used to simulate condensing flow through a nozzle instead of a 3-D simulation. Radial weighting factors were used to ensure that there are a sufficient number of simulated molecules for cells at small radial locations. Likewise species dependent weighting factors were used to ensure that there are comparable numbers of particles for each species in the computational domain. To reduce the computational cost of the statistical BGK method, supersonic flow is simulated past the nozzle throat (as shown in Fig. 1) assuming sonic state at the nozzle throat.

The computational domain used in our work is shown in Fig. 1. The domain is $\sim$6.3-by-0.75 nozzle diameters from the nozzle throat, *i.e.*, from x = 0 to 0.04 m and from y = 0 to 0.009 m. Table 3 provides additional information about the nozzle geometry. Before carrying out the condensation flow simulation, we simulated the non-condensing expanding flow through a nozzle. The recently implemented statistical BGK method for the 2-D axisymmetric DSMC code, SMILE [17], was used to simulate the gas expansion through the nozzle. We used a time step of 1×10^{-9} s, which is smaller than the local mean collision time and $\sim$15 million simulated particles, each of which represented 1×10^{9} gas molecules. The present work is computationally more challenging compared to the previous work [9] because ethanol, the condensible gas, is a trace species with air as the carrier gas. We have made use of the weighting scheme developed in the recent work [11] to simulate the flow conditions shown in Table 1 using a species weighting factor of 0.05 for the ethanol clusters.

We now present results for condensing flow of ethanol for different flow conditions. In all the figures, the abscissa represents distance from the nozzle throat normalized by the nozzle throat diameter. Temperature and pressure are normalized by their respective stagnation values. The LHS of Fig. 2 compares the variation of ethanol cluster to mixture mass fraction along the nozzle centerline obtained by the BGK method for different pressure cases. It can be seen that the numerical results agree well with the experiments. The RHS of Fig. 2 compares the ethanol cluster to ethanol gas mass fraction for the two cases. It can be seen that for both of the cases considered, almost all of the ethanol gas condenses to form ethanol clusters. The rate of gas to cluster conversion is highest in the beginning of the nozzle and decreases with distance from the nozzle throat. This occurs because, as the nozzle length increases, gas collisions are less likely to occur due to rarefaction. As shown in the LHS of Fig. 2, the point of condensation onset is predicted to be at approximately an x/D of $\sim$0.6 and x/D of $\sim$1.1 for the ethanol supply mass fractions of 0.008 and 0.005 respectively, showing fair agreement with experiments.

The LHS of Fig. 3 shows the cluster number density profiles obtained by the condensation model for different cases. It can be observed that for all of the cases, the cluster number density decreases after reaching a maximum value. This behavior occurs, because as clusters move through the flowfield, they have a tendency to merge with other gas and cluster particles that they collide with. Cluster particles can also evaporate because of the extra energy gained during a collision. These two effects along with the nucleation rate variation with gas number density result in the cluster number density profile as shown in the LHS of Fig. 3. Likewise, the RHS of Fig. 3 shows the cluster size profiles for different mass fraction cases considered. It can be seen that the cluster size increases along the plume centerline for all of the cases. This is expected, because as a cluster moves through the flowfield, it can consume gas particles or it can merge with other clusters, resulting in cluster growth. At the same time, the cluster size may decrease because of evaporation. Therefore cluster growth, coalescence, and evaporation affect the cluster size along its trajectory. All these effects become less significant further downstream as the flow expands. Accordingly, the figure shows that the cluster size, on a log scale, increases linearly initially with the axial distance for all of the cases, and then the rate of cluster growth slows for axial locations towards the end of the nozzle, i.e., at $x/D = 3.5$.

Now we discuss the effect of condensation on gas temperature and pressure profiles with respect to the non-condensing flow results. The latent heat release during the cluster growth processes results in increased thermal motion of the gas molecules. The increased thermal motion, in turn, elevates the rotational energy modes of monomers by collisions. The converse is true for the evaporation process due to latent heat removal. The LHS of Fig. 4 shows the BGK predicted variation of gas translational and rotational temperatures, normalized by flow stagnation temperature, along the nozzle centerline for the ethanol supply mass fraction of 0.005. As expected, the gas temperature increases due to the condensation of ethanol gas to clusters. Likewise, the RHS of Fig. 4 compares the pressure variation in a condensing flow with the non-condensing pressure variation for the ethanol supply mass fraction of 0.005. Pressure is normalized by flow stagnation pressure. It can be seen that the heat release due to the condensation process results in

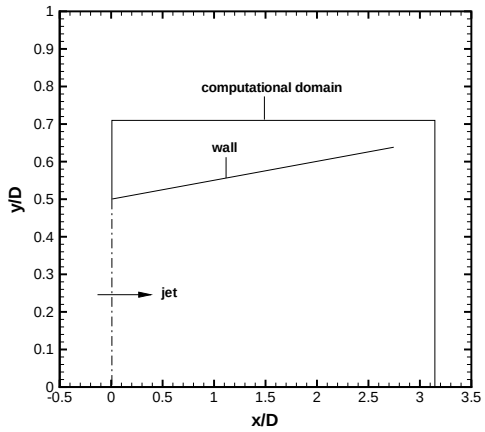

FIGURE 1. Computational domain used in the present work to simulate expanding flow through the nozzle. Note that the abscissa in this plot and subsequent ones represents distance from the nozzle throat normalized by the nozzle throat diameter.

a pressure rise.

CONCLUSIONS

Homogeneous condensing flow of ethanol through a nozzle was studied at a stagnation temperature and pressure of 296 K and 83.4 kPa respectively for two cases of ethanol supply mass fractions. The statistical BGK based condensation model, with the newly developed weighting scheme, was used to simulate the flow. These results were shown to agree well with the experimental data for all cases. It was shown that the use of the statistical BGK method allows the simulation of high density condensing flows, which was not possible with the use of the DSMC based condensation model.

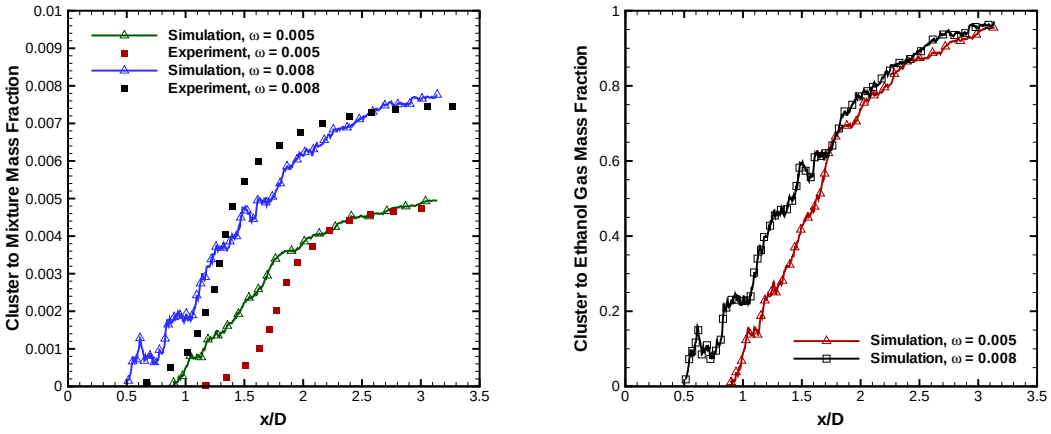

FIGURE 2. Comparison of centerline profiles obtained by the BGK method for condensing flow of ethanol for different cases, (LHS): cluster to mixture mass fraction; (RHS): cluster to gas mass fraction.

TABLE 1. Experimental Conditions

Case	ω	P_0 (kPa)	Ethanol Partial Pressure (kPa)	T_0 (K)
1	0.008	83.4	0.211	296
2	0.005	83.4	0.131	296

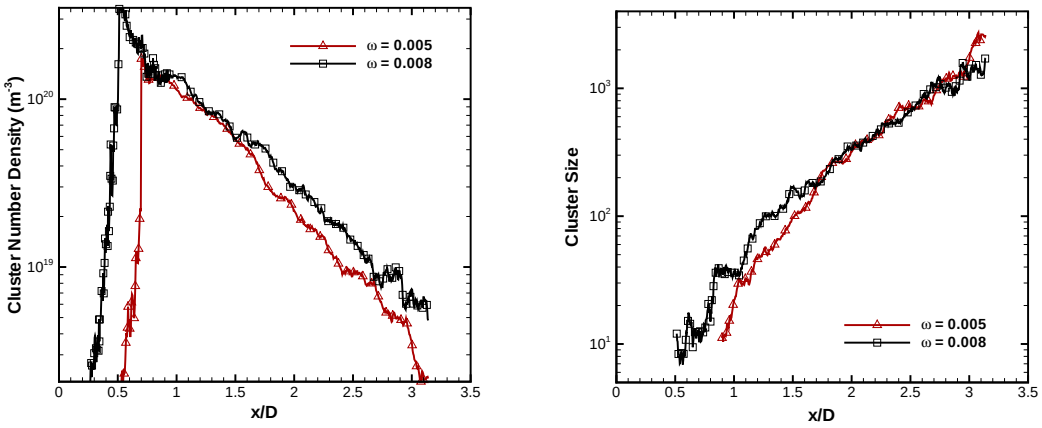

FIGURE 3. Comparison of centerline profiles obtained by the BGK method for condensing flow of ethanol for different cases, (LHS): cluster number density; (RHS): cluster size;

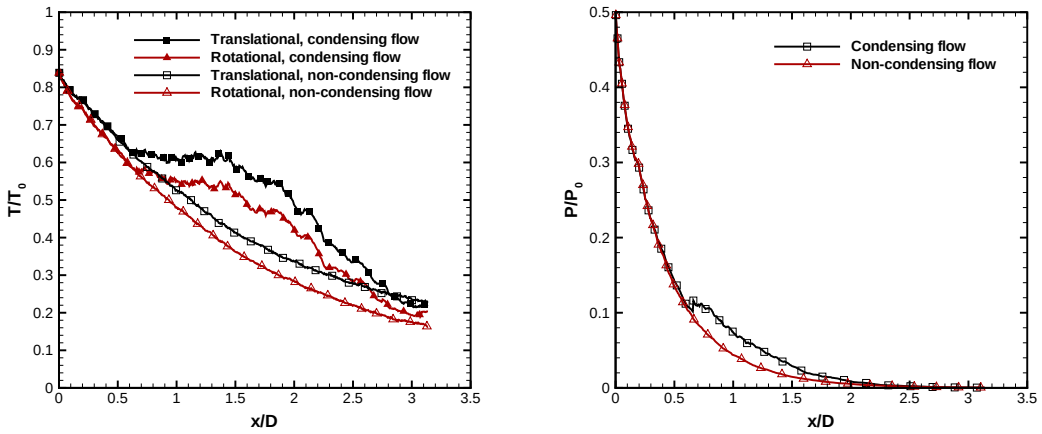

FIGURE 4. Comparison of centreline profiles between condensing and non-condensing flow for ethanol supply mass fraction of 0.005, (LHS): gas temperature; (RHS): gas pressure

TABLE 2. Ethanol Properties

Molecular Weight (g/mol)	46.07
Ratio of Specific Heats	1.13
Saturation Pressure (Pa)	133.32 ($10^{16.87-5819/T(K)+414300/T(K)^2}$), T(K) $<$ 219.1
	133.32 ($10^{9.760-2371/T(K)}$), T(K) $>$ 219.1
Surface Tension (J/m^2)	1.0E-03 (23.97 - 0.085 (T(K) - 273.15))

TABLE 3. Nozzle Geometry

Throat Radius (m)	6.373E-03
Exit Radius (m)	1.136E-02
Length of Divergent Section (m)	5.7E-02

ACKNOWLEDGMENTS

The research performed at the Pennsylvania State University was supported by the Air Force Office of Scientific Research Grant No. F49620-02-1-0104 whose support is gratefully acknowledged. We thank Professor M. Ivanov of the Institute of Theoretical and Applied Mechanics, Russia for the use of the original SMILE code.

REFERENCES

1. P. Wegener, J. Clumpner, and B. Wu, *The Physics of Fluids* **15**, 1869–1876 (1972).
2. A. C. Gallagher-Rogers, J. Zhong, and D. A. Levin, *Journal of Thermophysics and Heat Transfer* **22**, 695–708 (2008), ISSN 0887-8722.
3. W. C. Rochelle, E. A. Reid, T. L. Carl, and R. N. Smith, *AIAA Paper 2001-2813* (2001).
4. N. E. Gimelshein, R. B. Lyons, J. G. Reuster, and S. F. Gimelshein, *AIAA Paper 2007-1014* (2007).
5. V. N. Yarygin, V. G. Prikhodko, I. V. Yarygin, Y. I. Gerasimov, and A. N. Krylov, *Thermophysics and Aerodynamics* **10**, 269–286 (2003).
6. B. E. Wyslouzil, C. H. Heath, and J. L. Cheung, *Journal of Chemical Physics* **113**, 7317–7329 (2000).
7. F. Peters, *Journal of Chemical Physics* **77**, 4788–4790 (1982).
8. R. A. Zahoransky, and F. Peters, *Journal of Chemical Physics* **83**, 6425–6431 (1985).
9. R. Kumar, Z. Li, and D. Levin, *AIAA Paper 2010-818* (2010).
10. A. Ramos, J. M. Fernández, G. Tejeda, and S. Montero, *Physical Review A* **72**, 3204–3210 (2005).
11. R. Kumar, and D. Levin, *presented at 27th International Rarefied Gas Symposium, July 10-15, 2010, CA, USA* (2010).
12. M. Gallis, and J. Torczynski, The application of the bgk model in particle simulations, AIAA paper 2000-2360 (2000).
13. J. M. Burt, and I. D. Boyd, "Evaluation of a Particle Method for the Ellipsoidal Statistical Bhatnagar-Gross-Kroook Equation," in *44th AIAA Aerospace Science Meeting and Exhibit, AIAA Paper 2006-989, Reno, Nevada*, 2006.
14. R. Kumar, E. Titov, D. Levin, N. Gimelshein, and S. Gimelshein, *AIAA Journal* **48**, 1531–1541 (2010).
15. R. Kumar, E. Titov, and D. Levin, *Journal of Thermophysics and Heat Transfer* **24** (2010).
16. R. Kumar, E. Titov, D. Levin, N. Gimelshein, and S. Gimelshein, *Journal of Thermophysics and Heat Transfer* **24**, 254–262 (2010).
17. M. S. Ivanov, A. V. Kashkovsky, S. F. Gimelshein, G. N. Markelov, A. A. Alexeenko, Y. A. Bondar, G. A. Zhukova, S. B. Nikiforov, and P. V. Vashenkov, "SMILE System for 2D/3D DSMC computations," in *Proceedings of the 25th International Symposium on Rarefied Gas Dynamics*, edited by M. S. Ivanov, and A. K. Rebrov, Publishing House of the Siberian Branch of the Russian Academy of Sciences, Novosibirsk, 2007, pp. 539–544.
18. E. Titov, R. Kumar, and D. Levin, *AIAA Paper 2009-3756* (2009).